World Academy of Science, Engineering and Technology
International Journal of Pharmacological and Pharmaceutical Sciences
Vol:9, No:11, 2015

ATR-IR Study of the Mechanism of Aluminum Chloride Induced Alzheimer's Disease; Curative and Protective Effect of *Lipidium sativum* Water Extract on Hippocampus Rats Brain Tissue

Maha Jameal Balgoon, Gehan A. Raouf, Safaa Y. Qusti, Soad Shaker Ali

***Abstract*—**The main cause of Alzheimer disease (AD) was believed to be mainly due to the accumulation of free radicals owing to oxidative stress (OS) in brain tissue. The mechanism of the neurotoxicity of Aluminum chloride ($AlCl_3$) induced AD in hippocampus Albino wister rat brain tissue, the curative & the protective effects of *Lipidium sativum* group (LS) water extract were assessed after 8 weeks by attenuated total reflection spectroscopy ATR-IR and histologically by light microscope. ATR-IR results revealed that the membrane phospholipid undergo free radical attacks, mediated by $AlCl_3$, primary affects the polyunsaturated fatty acids indicated by the increased of the olefinic -C=CH sub-band area around 3012 cm^{-1} from the curve fitting analysis. The narrowing in the half band width (HBW) of the νCH_2 sub-band around 2852 cm^{-1} due to Al intoxication indicates the presence of trans form fatty acids rather than gauch rotomer. The degradation of hydrocarbon chain to shorter chain length, increasing in membrane fluidity, disorder, and decreasing in lipid polarity in $AlCl_3$ group indicated by the detected changes in certain calculated area ratios compared to the control. Administration of LS was greatly improved these parameters compared to the $AlCl_3$ group. Al influences the Aβ aggregation and plaque formation, which in turn interferes to and disrupts the membrane structure. The results also showed a marked increase in the β-parallel and antiparallel structure, that characterize the Aβ formation in Al-induced AD hippocampal brain tissue, indicated by the detected increase in both amide I sub-bands around 1674, 1692 cm^{-1}. This drastic increase in Aβ formation was greatly reduced in the curative and protective groups compared to the $AlCl_3$ group and approached nearly the control values. These results supported too by the light microscope. $AlCl_3$ group showed significant marked degenerative changes in hippocampal neurons. Most cells appeared small, shrieked and deformed. Interestingly, the administration of LS in curative and protective groups markedly decreases the amount of degenerated cells compared to the non-treated group. In addition, the intensity of congo red stained cells was decreased. Hippocampal neurons looked more/or less similar to those of control.

This study showed a promising therapeutic effect of *Lipidium sativum* group (LS) on AD rat model that seriously overcome the signs of oxidative stress on membrane lipid and restore the protein misfolding.

***Keywords*—**Aluminum chloride, Alzheimer's disease, ATR-IR, *Lipidium sativum*.

Gehan A. Raouf, Safaa Y. Qusti, and Maha Jameal Balgoon are with the Department of Biochemistry, Faculty of Science, King Abdulaziz University, Jeddah, KSA (Corresponding author: Gehan A. Raouf, phone: +966508493291; fax: +966126402000; e-mail: gehan_raouf @hotmail.com, safaaqusti@yahoo.com, e-mail: mbalgoon@ kau.edu.sa).

Soad Shaker Ali is with Saudi Arabia-Jeddah Faculty of Medicine (e-mail: soadshaker@gmail.com).

I. Introduction

ALZHEIMER'S DISEASE (AD) is the most common form of dementia in the old age that slowly destroys neurons. AD is a progressive neurodegenerative disorder [1]. Currently, AD affects nearly 5% of people 65-year old and over 30% of those 85-year old, affecting more than 27 million people in the developed world [2]-[4]. AD is characterized by atrophy of cerebral cortex and selective neuronal damage in the hippocampal brain tissues.

Oxidative damage and the formation of free radicals may occur for several reasons such as exposure to chemicals, metals, irradiation and toxins causing to lipid peroxidation, which in turn affects the activities of protective enzymatic antioxidants that are greatly sensitive indicators of increased oxidation reactions [5]. When lipids attacked by free radicals, the lipid peroxidation chain reaction proceed [6]. This lipid degradation reaction leads to broken chemical bonds, cross-linkages, and conformational changes of many bio molecular compounds. The pathological hallmarks of AD are known to be the deposition of extracellular Aβ plaques, the formation of intracellular neurofibrillary tangles (NFTs) (highly phosphorylated tau proteins), and the selective loss of synapses and neuron, which lead to neural death in the hippocampal and cerebral cortical regions [7].

Aluminum compound is a well-known neurotoxin, and it has a great affinity to bio-membrane and the ability to promote formation and aggregation of insoluble Aβ [8]. Various neurodegenerative diseases such as AD and Parkinsonism disease are strongly linked to Al [7]. Aluminum can bind to different metal binding proteins such as Ca, Fe, Cu and Zn that accordingly influences homeostasis of other metals [7]. Aluminum may exert its neurotoxicity via free radical production and peroxidation damage to lipids and proteins [9]. Chronic aluminum exposure has a great affinity to bio-membrane and the ability to promote formation and aggregation of insoluble Aβ plaques and (NFTs) in Alzheimer brain. References [10]-[13] proved that Al exposure is associated with impairment of mitochondrial functions, *in vivo* and *in vitro*, as well as the antioxidant defense system. Al decreases the antioxidant enzyme status [14], [15]. Aluminum can cause also a disturbance in the enzyme activity involved in acetylcholine metabolism and leads to cognitive dysfunction [16], [17].

The treatment available now for AD are not able to stop the malfunction and death of neurons [2], [18]. Available drugs on the market now include inhibitors of acetyl cholinesterase such as tacrine, donepezil, rivastigmine, and galantamine [19]. The use of traditional medicine is widespread and plants represent a large source of natural antioxidants that might serve as leads for the development of novel drugs [20]. Usually, medicinal plants with antioxidant activities have been used in the treatment of several human diseases, cancer, cardiovascular and neurodegenerative diseases such as AD [21].

The purpose of this study conducted to investigate the mechanism of $AlCl_3$ neurotoxicity, the curative and protective effect of the medicinal plant LS water extract in rat models. The hippocampus rat brain analyzed spectroscopically by attenuated total reflection spectroscopy (ATR-IR) to study the alteration at sub molecular levels, in lipid and protein conformational structure and histologically by light microscope.

II. Materials and Method

The experimental work of the present study was conducted at the King Fahd Medical Research Center, Medical Biophysics Laboratory at King Abdulaziz University, Jeddah, Saudi Arabia.

A. Chemicals

Aluminum chloride in formed white powder, and all chemicals, in the present study were in the pure form purchased from Sigma Aldrich chemical company, St. Louis, USA supplied.

Lipidium sativum group (LS) seeds were obtained from the local herbalist shops in Jeddah. The type obtained was grown in Al-Qaseem area in Saudi Arabia was grown in Al-Qaseem area in Saudi Arabia.

B. Animal and Experimental Design

One hundred albino wister male rats with a body weight ranged between 200 to 250 gm. were housed in plastic cages in a room with a relative humidity of 70%, temperature of (24±1°C), and exposed to a light and dark cycle of 12 h duration. The rats were acclimatized for one week before the experiment started. The current study was approved by the Animal House, King Fahd Medical Research Center, King Abdulaziz University. Five groups of rats with a minimum of 20 rats per each were sorted randomly. Control (Cont) group G1, G2: AD group ($AlCl_3$), G3: curative group (Cure), G4: protective group (Prot), and G5: positive control group (LS). AD was induced to rats by administration of ($AlCl_3$) intraperitonealy (IP) (10 mg/kg of body weight) daily to groups 2, 3, 4 group; 1, 5 were injected (IP) normal saline instead. Groups 3, 4, 5 were receiving orally 20 mg/kg of body weight LS water extract while groups 1, 2 were receiving orally normal saline. All rats received standard rat pellet form Grain Silos and Flour Mills Organization, Jeddah, Saudi Arabia and water as beverage. Diet and water were supplied ad-libitum.

C. Brain Tissue Sampling and Preparation

Three rats from each group were fasted overnight, then the rats were euthanized following light ether anesthesia. The skull was opened carefully and the whole brain of each rat was rapidly removed. The brain was quickly dissected into 2 halves; one was fixed in 10% neutral buffered formalin for further histopathological examination. Hippocampus from the other half was dissected out accord to procedure documented by [22]. The hippocampus tissues washed with saline, immediately immersed in eppendorf tubes in liquid nitrogen and stored at −80°C until use. All samples were lyophilized, and grounded in agate mortar prior to ATR-IR measurement.

D. Attenuated Total Reflection

For each sample (ATR-IR) spectrum was recorded in absorbance form using Perkin Elmer Spectrum 100 instrument. The spectrum was obtained in the wavenumber range of 4000-400 cm^{-1} with an average of 40 scans and spectral resolution of at 4 cm^{-1}. All the samples were baseline corrected and normalized to the entire spectrum by using OMNIC software program disc in order to increase the resolution of the overlapping bands before any measurements. Based upon the findings described for the previous specimen, a Gaussian decomposition was used to localize the position of the bands in the row spectra. Background spectra, which were collected under identical conditions, were subtracted from the sample spectra automatically. For each examined sample, the final spectrum was represented by co-added the three spectra as the average of three different measurements. The parameter studied was proteins and lipids.

E. Histopathological Examination

Tissues fixed in neutral buffered formalin (10%) were further processed for cleared in xylene and embedded in paraffin embedding in a hot air oven at 561^{o}C for 24h. Paraffin bees wax blocks were prepared for sectioning at 4mm using a microtome. Five-micron sagittal sections of brain tissue were stained with hematoxylin and eosin stains for general structure and Congo red for amyloid substance. Histopathological changes were evaluated using a light microscope [23].

III. Result

The average IR spectra taken from three different rat brain hippocampus tissue obtained from each group. Each spectrum was baseline corrected, normalized and co-added (Fig. 1). The main IR absorption bands that belong mainly to lipids, proteins, carbohydrates, and nucleic acids, together with their band assignments are given in Table I according to the literature. Detailed spectral analysis will be discussed here, into two distinct frequency ranges namely, (C-H stretching region) Symmetric and a Symmetric stretching of methyl (CH_3) and ethylene (CH_2) functional groups [3030-2800 cm^{-1}], and 1800-900 cm^{-1} region that comprise mainly the ester carbonyl (C=O) group and the amide I and amide II bands. Carful inspection of the IR spectra revealed that there are no obvious changes among the 5 groups under investigation apart

from slight changes in the band intensities and frequencies shift.

In order to investigate the qualitative and quantitative changes in the lipid profile, and the protein secondary structure of the hippocampus brain tissues, the second derivates was carried to these distinct regions (data not shown). A detectable changes in the peak intensity, appearance and disappearance of new sub band, were observed among the groups under investigation compared to the control.

According to the second derivative analysis and in order to segregate between the overlapped bands and to explore more changes between the spectra of the tested groups, curve fitting of the average spectrum taken from each group was obtained to the same examined regions as shown in Figs. 2 (a) and (b).

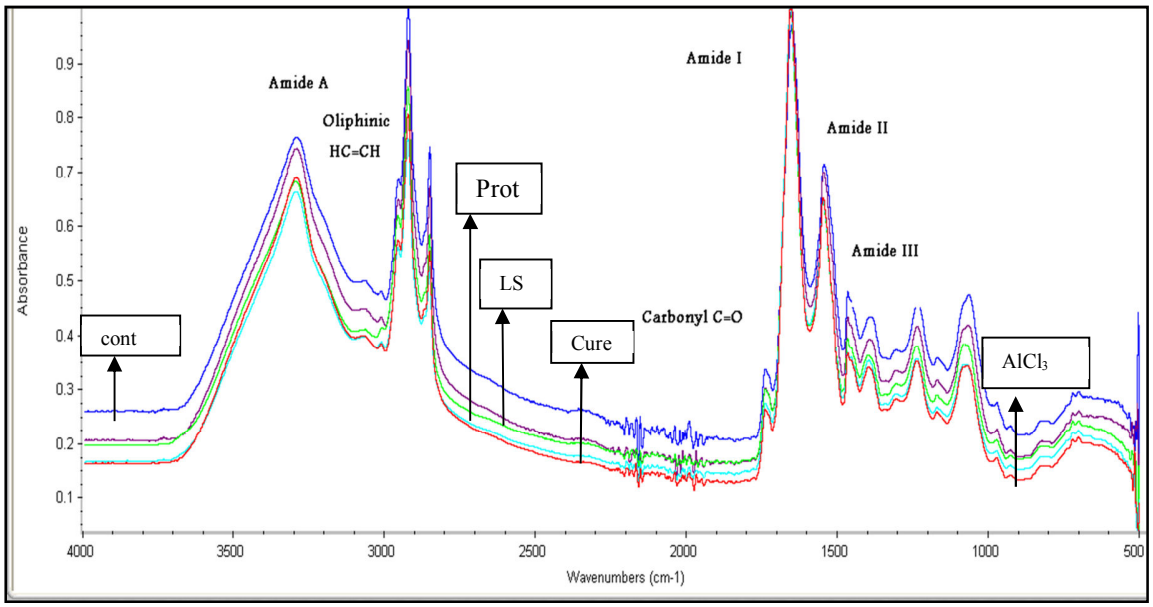

Fig. 1 The ATR-IR spectra of rat hippocampous brain tissue (cont, $AlCl_3$, Cure, Prot, and LS groups) in region (4000-500 cm^{-1}). Each spectrum is the average of three different measured spectra

A. ATR-IR Results

1. The Region 3050-2800 cm^{-1}: Symmetric and Asymmetric Stretching of Methyl (CH_3) and Methylene (CH_2) Functional Groups

The spectroscopic measurement of C-H vibrations of lipids hydrocarbon chain was found, so the peak position, intensity, HBW, and area were given in Table II.

A drastic increase in the olefinic band area near 3012 cm^{-1} for both the $AlCl_3$ and all LS treated groups compared to the control was detected. Meanwhile, the maximum increase in this band area was recorded in the protective group. For the olefinic band around 3012 cm^{-1}, the HBW of this band decreased drastically in the $AlCl_3$ group compared to the control. Treating rats with LS water extract leads to a marked increase in HBW in both the curative and protective groups than the $AlCl_3$ group but its value is still lower than that detected in the control group.

The area of the CH_2 symmetric stretching is slightly decreased from the control 5.683 to 5.39 in the $AlCl_3$ group. For all LS treated groups these areas markedly decreased and the minimum value was recorded in the curative group compared to the control. Although the HBW of this band decreased only in the $AlCl_3$ group and obviously increased in the other LS treated groups compared to the control. For the asymmetric stretching vibrations mode of the CH_2, the band intensity, the HBW, and the area were all increased in the $AlCl_3$ group compared to the control. While, these parameters were all decreased instead in the LS treated groups except in the LS group, which shows a slight increase in the HBW value than the control. The same behavior was detected for the sCH_3 stretching band apart from a slight increase in the values of the HBW only in the $AlCl_3$ and protective groups compared to the control.

The asymmetric stretching of the CH_3 band by contrast showed a significant increase in these band areas in all tested groups compared to the cont. However, there are a drastic increase in this half band, which observed only in the LS treated groups compared to both the control and $AlCl_3$ groups. The frequency of the CH_2 stretching band around 2924 cm^{-1} can determine the degree of the membrane rigidity. The higher frequency is the higher the membrane fluidity [25].

This band showed a negligible shift towards the lower frequency in case of $AlCl_3$ group only by contrast a considerable band shift in this band towards the higher frequencies were detected in all LS treated groups and the maximum shift was detected in the curative group.

TABLE I
PROPOSED ASSIGNMENTS OF THE FTR-IR SPECTRA OF HIPPOCAMPUS RAT BRAIN TISSUE IN THE (3030-500) CM^{-1} SPECTRAL RANGE [24]

Wave number (cm^{-1})	Band assignments
3293.6	Amide A: mainly ν =N–H stretching of proteins
3065	Amide B: N–H stretching of proteins
3013.47	Olefinic HC=CH stretching of alkene: lipids
2956	vas (CH_3)mainly lipids, proteins
2923	νas (CH_2) mainly lipids, proteins
2852.38	νs (CH_2) mainly lipids
1739.81	Carbonyl C=O stretch: lipids
1651.42	Amide I: ν (C=O), ν (C-N), δ (H-N)
1545.33	Amide II:, ν =(C-N), δ (H-N) of polyproteins
1466.55	CH_2 δs: mainly lipids
1388	νs (C=O):lipid, proteins (fatty acids and amino acids)
1307.36	Amide III:(N-H), (C-H) band components of proteins
1234.95	νas PO_2^-:asymmetric stretch: mainly phospholipids
1170.32	νas $(COOC)^-$: phospholipids, triglycerides and cholesterol esters
1066.11	νs PO_2^-:nucleic acids; ν (HO–C–H): carbohydrates
972.85	ν:C-O;δ C-N -C stretch: nucleic acids, Fingerprinting region: mainly nucleic acid.

ν: stretching vibrations, δ: bending vibrations, s: symmetric, as: asymmetric

Ratios of some specific infrared sub-bands have been evaluated for quantitative comparison between the control and the treated groups. Using the curve fitted FTIR data, the following area ratios were calculated [Table III]. The νas(CH_2)/νs(CH_3) is used as a measurement of environmental polarity as it increases with the polarity of lipid chains environment. This ratio decreased only for the $AlCl_3$ group compared to the control while, it increased dramatically for all LS treated groups compared to the control. The νs(CH_2)/νs(CH_3) ratio is correlated with the looseness of lipid chains packing and the νas(CH_2)lipids/total lipid ratio which indicates the alterations in phospholipids chain length were also calculated. These ratios showed a significant increase in their values in all tested groups compared to the control indicating high lipid disorder and a degradation of the fatty acid acyl chain to shorter hydrocarbon chain length respectively in all tested groups. The maximum value was detected for $AlCl_3$ group compared to the control. The Carbonyl ester/total lipid ratio was also used to study the carbonyl status in the system. This ratio showed a marked increase in all tested groups compared to the control; the maximum value detected in curative group. To investigate the degree of unsaturation of phospholipids fatty acids, νs (CH)/νas (CH_3) area ratio is determined. The value of A (3012) cm^{-1}/A (2956) ratio increased in all treated groups compared to the control.

2. The Region 1800-1500 Cm^{-1} Analysis of Amide I, II, III, and Carbonyl Bands

The carbonyl band around 1740 cm^{-1} upon curve fitting [Table IV] gives 6 discrete sub-bands for the control while it gives 5 sub-bands in case of $AlCl_3$ group with complete absence of the sub-band around 1728 cm^{-1}. Meanwhile, this band, for all LS treated groups, gives only four distinct sub-bands with complete absence of 1720, 1736 cm^{-1} sub-band previously detected in the control. The table also gives information about the shift in the position of these sub-bands for all tested groups compared to the control.

A drastic increase in the HBW and areas of all the carbonyl sub-bands for LS treated groups over the control were also detected. The same observation was also noticed for the AlCl3 group compared to the control but the increase in the HBW and the area were much lower than that observed for the LS groups. Moreover, a little decrease in the HBW of the sub-bands around 1712, 1722 cm-1 were recorded instead of the previously increase described.

The carbonyl status of the system and the weight of formation of carbonyl compounds against lipase action or lipid degradation during lipid oxidation were evaluated by measuring C=O/amide II & C=O/total lipid area ratios.

The values of these ratios increase dramatically in AlCl3 group and all LS treated groups as well (data not shown). It should be mentioned here that the increase of these ratios were vigorously in curative and protective groups particularly.

TABLE II
WAVE NUMBERS, INTENSITIES, HBW, AND AREAS OF THE REGION 3030-2800 CM^{-1}

Groups	Wave Number (cm^-1)	Intensity	HBW	Area
	2852.317	0.3007	17.757	5.6831
	2873.33	0.1453	20.294	3.1384
Control	2924.267	0.524	28.875	16.1062
	2956.653	0.2057	23.716	5.1933
	3012.296	0.0041	14.779	0.0647
	2852.343	0.3109	16.283	5.3893
	2872.271	0.1663	20.308	3.5953
$AlCl_3$	2924.155	0.5653	29.54	17.7755
	2957.199	0.2399	23.814	6.082
	3012.386	0.0143	12.351	0.1881
	2852.869	0.2085	18.333	4.0683
	2874.135	0.1108	20.528	2.4218
Curative	2925.496	0.4318	28.779	13.2266
	2959.373	0.2066	27.101	5.9606
	3012.279	0.014	14.77	0.2195
	2852.829	0.256	18.296	4.985
	2871.839	0.1268	16.344	2.2061
Protective	2925.07	0.5072	28.957	15.6351
	2959.368	0.2423	28	7.2218
	3010.283	0.0182	12.211	0.2366
	2852.759	0.2362	18.564	4.6676
	2872.352	0.1104	16.835	1.9775
LS	2924.279	0.4649	28.424	14.0655
	2958.562	0.2156	28.95	6.6439
	3012.507	0.0101	13.656	0.1465

The Amide II/Amide I ratio which give information about the changes in the nucleic acids was calculated and revealed that this ratio was decreased in all tested groups compared to the control. The minimum value was detected in the curative group.

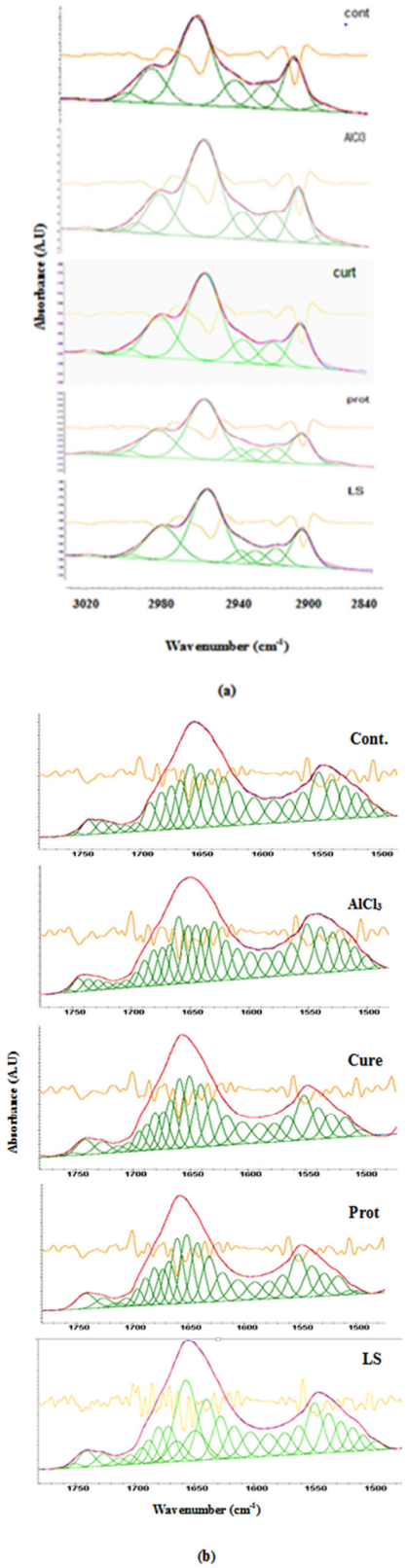

Fig. 2 (a) Curve fitting of hippocampus brain tissues of cont., $AlCl_3$, Cure., Prot., and LS groups in the IR (3030-2800 cm^{-1}); (b) Curve fitting of the amide I and amide II bands of the hippocampus brain tissue taken from cont., $AlCl_3$., Cure., Prot., and LS groups at the range (1800-1500 cm^{-1})

To evaluate the total lipid to protein ratio the area of [CH2 (2924 cm-1) + CH2 (2852 cm-1)] to [(Amide I + Amide II)] was calculated (data not shown). The lipid to protein ratio decreased in all tested group compared to the control and the minimum decrease was detected in the curative group. The vales were 0.363, 0.317, 0.235, 0.297 and 0.253 for cont, AlCl3, Cure, Prot, and LS groups respectively. For further investigation of the amide I region near 1652cm^{-1} which gives the information about the whole protein secondary structure of the cell, the percentage area of the protein sub-bands and the sub-band position together were calculated (data not shown).

TABLE III
FTR-IR AREA RATIOS QUANTITATIVE MEASUREMENTS OF PROTEIN CONTENT, LIPID CHAIN PACKING, AND CARBONYL ESTER FORMATION IN RAT BRAIN TISSUE

Area Ratios/Groups	Cont	$AlCl_3$	Cure	Prot	LS
$vas(CH_2)/vs(CH_3)$ Polarity	5.132	4.9441	5.4615	7.0872	7.113
looseness of lipid chains packing $vs(CH_2)$ lipid/ total lipid)	1.8108	1.499	1.6799	2.2596	2.527
phospholipids chain length Carbonyl ester/Total lipid	0.6953	0.7673	0.7648	0.7582	0.751
Carbonyl status of the system $vas(CH)/vas(CH_3)$	0.1592	0.1926	0.285	0.233	0.235
Unsaturated phospholipids	0.0125	0.0309	0.0368	0.0327	0.022

It should be mentioned here that the α-helix band around 1652 cm^{-1} is clearly resolved into two distinct α-helix sub-bands around 1651 and 1659 cm^{-1}. The β-sheet protein sub-band around 1629.5 in the cont. and LS group was shifted towards the higher frequency in all AD groups which comprise ($AlCl_3$, cur. and pro. groups) compared to the control and LS groups. Another valuable shift in the α-helix sub-band was detected for the control, cur, pro, and LS groups in opposition to $AlCl_3$ group. The sub-band centered at 1651.9, 1650.9, 1651.4, and 1650.7 cm^{-1} respectively. While, this sub-band shifted towards the lower frequency only in the $AlCl_3$ group, it appeared at 1649.9 cm^{-1}. A spectacular shift in the β-sheet protein sub-band was also detected in $AlCl_3$ group towards the higher frequency at 1674.3 cm^{-1} compared to the control at 1673.6 cm^{-1} and the other LS tested groups (1673.5, 1672.7 and 1672.9 cm^{-1} for curative, protective, and LS respectively. By contrast, a marked shift in the β-anti-parallel pleated sheet protein sub-band centered at 1695.8 cm^{-1} for the control group towards the lower frequency at 1692.2 cm^{-1} for the $AlCl_3$ group was recorded. This shift was not significant for the other LS treated groups compared to the control.

3. Statistical Analysis

Further differences among the groups under investigation were recorded by using cluster analysis. The multivariate classification (data recognition) was performed between the intensities of the collected IR bands Fig. 3 cluster analysis. Interestingly, all tested groups were well differentiated. Moreover, the dendrogram strongly differentiated between all LS treated groups on one side and both the control and $AlCl_3$ groups on the other side. Furthermore, LS and Protective

groups were significantly differentiated than the curative group.

The control and $AlCl_3$ groups were strongly segregated as shown in the dendrogram.

TABLE IV
WAVE NUMBERS, INTENSITIES, HBW, AND AREAS OF THE REGION 1700-1750 CM^{-1}

Groups	Wave Number (cm^{-1})	Intensity	HBW	Area
Control	1704.53	0.0431	10.176	0.4672
	1712.14	0.0324	10.223	0.3526
	1720.92	0.0407	10.18	0.4414
	1728.52	0.0569	10.223	0.6197
	1736.74	0.0669	10.257	0.7309
	1745.28	0.0747	10.775	0.8565
				3.4683
$AlCl_3$	1703.28	0.0677	10.219	0.7365
	1712.2	0.0539	9.841	0.5646
	1722.4	0.0669	9.898	0.7044
	1732.34	0.0914	10.881	1.0591
	1743.68	0.109	12.056	1.3982
				4.4628
Curative	1703.95	0.0645	12.153	0.8346
	1712.81	0.0487	13.564	0.7032
	1726.95	0.0847	15.966	1.4399
	1741.89	0.1099	16.672	1.9508
				4.9285
Protective	1705.69	0.0619	12.051	0.7946
	1713.72	0.0312	13.756	0.4569
	1726	0.0706	16.562	1.2445
	1742.02	0.1095	19.811	2.3095
				4.8055
LS	1704.61	0.0648	11.391	0.7852
	1713.94	0.0492	12.439	0.6519
	1726.82	0.0822	13.919	1.2181
	1740.82	0.1085	15.138	1.7479
				4.4031

B. Histological Results

1. Haematoxylin and Eosin Stain for General Structure

Fig. 4 showed that in $AlCl_3$ animal model of AD degenerative changes were observed in hippocampal neurons compared to normal cells of the control. Most cells appeared smaller, shrinked and deformed. They have dark cytoplasm and small dark (pyknotic) nuclei. By contrast, in the curative group where LS extract was given 4 weeks after $AlCl_3$ administration there was marked decrease in degenerated cells compared to non-treated group. Meanwhile, in the protective group, administration of $AlCl_3$ together with LS water extract result also in marked protection against neuronal degenerative changes induced by $AlCl_3$ in AD model. However, LS water extract given alone did not alter the normal structure of hippocampal neurons. Even neuronal population became more numerous and cells looked normal with vesicular lightly stained nuclei.

2. Congo red Stain for Amyloid Substance

Compared to the control (Fig. 5) showed that, the hippocampal tissue of the AlCl3 group demonstrated that degenerated neurons deeply stained by Congo red. This is indicating the deposition of amyloid substance within the cytoplasm and nuclei of affected neuron. In hippocampus neurons of animals administrated LS water extract either after 4 weeks of $AlCl_3$ administration (curative group) or early together with $AlCl_3$ (protective group), less neurons showed such deposition and most looked similar to control with more protection in curative group. In LS group, staining of cells was similar to the control group.

IV. DISCUSSION

The mechanism of cytotoxicity and/or neurotoxicity of many compounds are thought to be mainly due to the oxidative stress involved in the production of reactive oxygen species (ROS), that include superoxide anion, hydrogen peroxide, superoxide radical and hydroxyl radical [26], [27]. The degree of oxidative damage is depended on the balance between the oxidative stress and the efficiency of the antioxidant mechanism that found in the majority of cells [28].

In general, brain tissues are highly susceptible to be attacked by free radicals, which is produced here in this study by AlCl3, due to its highly unsaturated lipid content especially in the axonal layer in hippocampus (white matter) than the cortical region (grey matter), its high rate of oxidative metabolic activity, and its low level of antioxidant enzymes [29].

Many studies suggested that upon lipid peroxidation, due to oxidative damage and free radicals production, the concentration of polyunsaturated fatty acids decreased and the concentration of saturated fatty acids increased. This is due to the fact that free radicals attack mainly the double bond sites of unsaturated fatty acids owing to lipid peroxidation [30], [31].

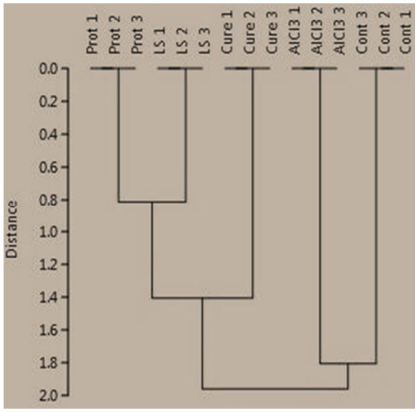

Fig. 3 HCA spectral analysis of the two regions of the hippocampus brain tissue taken from cont., $AlCl_3$, Cure, Prot., and LS groups

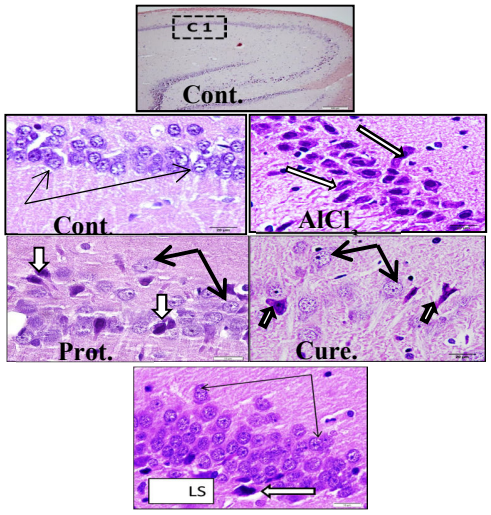

Fig. 4 Sections in rat hippocampus stained by H & E red for general structure from different experimental groups G1: control. G2.AD ($AlCl_3$) G3.Curative (AD then LS).G4. Protective (AD +LS. G5.LS showing that $AlCl_3$ induced degenerative changes in hippocampal neurons where cells (arrows) looked shrinked and dark stained (apoptotic cells). LS water extract either given after 4 weeks of AD induction (G3) or together with AlCl4 (G4) result in preservation of neuronal normal structure with marked decrease in apoptotic cells (arrows)

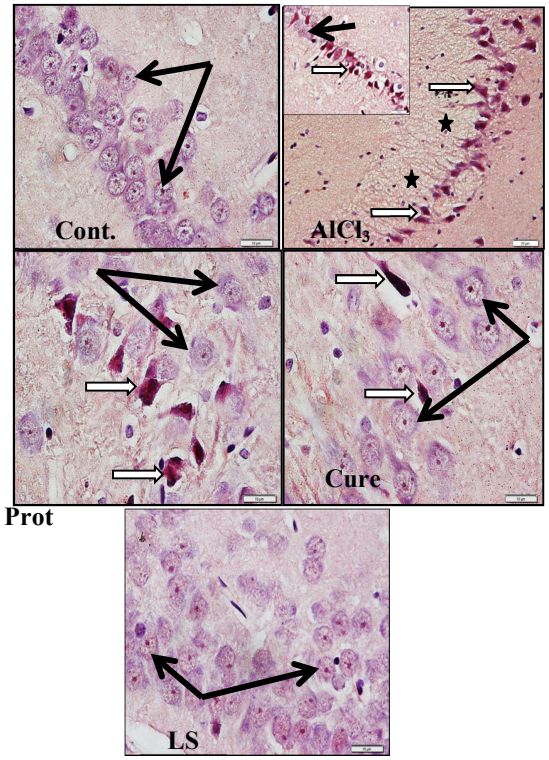

Fig. 5 Sections in rat hippocampus stained by Congo red for amyloid substance from different experimental groups G1: control. G2.AD ($AlCl_3$) G3.Curative (AD then LS).G4. Protective (AD+LS. G5.LS showing negative staining in control group, increase in staining of degenerated neurons of AD group, decrease intensity of staining in both curative and protective groups with good response in the curative. In LS group, the staining is similar to control

The olefinic band HC=CH around 3012 cm^{-1} is usually used to measure and monitor the degree of phospholipids acyl chain saturation or unsaturation due to oxidative stress. To examine the lipid content and profile of the hippocampus rat brain tissue specific area band ratios were calculated and evaluated. The olefinic to CH_3 area ratio [A (3012 cm^{-1})/ A (2956 cm^{-1})] is a good indicator for testing the unsaturated level of the system. The lipid to protein ratio [A (2924+2852) cm^{-1}/A (amide I+ amide II)] can also give information about the lipid and protein asymmetry, which is greatly related to membrane function [29]. The ester carbonyl to total lipids [A(1700-1750 cm^{-1})/ A(2924+2852) cm^{-1}] was used to examine the carbonyl content of the system, [A(2924) cm^{-1}/ A(2873) cm^{-1}, 2924cm^{-1} /2924+2852 cm^{-1} &2924 cm^{-1} /2852 cm^{-1}] were used to examine membrane lipid polarity, hydrocarbon chain length and ordering respectively.

For the AlCl3 group, the unexpected marked increase in the sub-band area of the olefinic band together with the observed increase in [A(3012 cm^{-1})/A(2956 cm^{-1})] ratio compared to the control may be attributed to the increase in the unsaturated to saturated lipids in the hippocampus membrane tissue mediate by $AlCl_3$ toxicity. These increase may also referred to accumulation of lipid peroxidation end products [6], [32].

Lipid peroxidation is a complicated process. When source of free radicals attack biological membrane or tissue a series of chain reaction takes place and polyunsaturated fat acids are particularly the targets that undergo oxidation yielding lipid hydroperoxide and dialkylperoxides which are known as primary lipid peroxidation products [33]. Rearrangement of double bonds in lipid oxidized membrane or tissue to form conjugated dienes occurs when lipid acyl chains contain more than one double bond. A variety of secondary lipid peroxidation products, such as alkanes, carbonyl compounds, lipid aldehydes and alkyl radicals, occurs as a result of hydroperoxides decomposition through complex propagative reactions [33], [34]. Thus, the increased olefinic band area and -3012 cm^{-1}/2956 cm^{-1} ratio is believed now to be due to the accumulation of lipid peroxidation end products. This finding is also supported by the detected considerable decreased in (A2924 cm^{-1}/A2873 cm^{-1}) ratio that used for lipid polarity evaluation. The decrease in this ratio may reveal the weakened in the Van der Waal forces among the polar head groups of the membrane phospholipids and consequently an increase in the membrane fluidity and membrane disorder should happen. This is evident by the examination of (A2852 cm^{-1}/A2873 cm^{-1}) and (A2924 cm^{-1}/A (2924+2852) cm^{-1}) ratios. These ratios showed a considerable decrease in the lipid chain packing and an increase in the phospholipids chain length ratio respectively, the increase in this ratio is an indicator of the length of acyl chain length which contain then large amount of short chain fatty acids [6], [32]. Moreover, oxidation may result in membrane disordering and subsequent increase in the HBW of the CH stretching bands. The behavior of the CH stretching vibration of the hydrocarbon chains upon lipid oxidation can give a good method for peroxide determination [35].

In the present study, the observed band shift in the asνCH_2

around 2922 cm^{-1} to the higher frequency in both $AlCl_3$ and all LS treated groups considered as an indicator for the increased membrane fluidity. The higher shift was detected for the curative group. In curve fitting analysis, this band shift to higher frequency was more apparent for both the curative and protective groups. The shift was negligible between cont. $AlCl_3$ and LS groups (2924.27, 2924.16, 2925.5, 2925.07 and 2924.28 cm^{-1}).

The $svCH_2$ around 2852 cm^{-1} was used to estimate the content of trans and gauche rotomers in hydrocarbon chains. The lower frequencies and narrowing of the HBW of the $svCH_2$
higher hydrocarbon chain order and hence higher trans content [36]. Van der Waal's interactions between the lipids are at their maximum [37]. In this study, the marked decrease in the HBW of the $svCH_2$ band and a slight band shift of the $asvCH_2$ band at 2924.27 cm^{-1} in the cont. to lower frequency at 2924.16 cm^{-1}, of the CH region decomposition, upon Al intoxication may attributed to the change of the hydrocarbon chain to more trans rotomers than gauche rotomers. However, by contrast with [37], there were a decrease in both membrane ordering and van der Waal forces indicated by the decrease in the lipid polarity and lipid chain packing area ratios. The increase in membrane fluidity and disorder may referred to the fact that mentioned earlier in AD brain tissue, Aβ can disrupt the membrane fluidity which can contributing to the disruption in different cell functions such as calcium signaling and lipid transport [38]-[40].

Aβ is resulting from the membrane-bound amyloid precursor protein (APP), the oligomeric Aβ forms pore-like structures in lipid membrane that disrupt ion homestasis and cause (apoptosis) [41].

Koppaka & Axelsen [42] showed that membranes contain oxidative damaged phospholipids can accumulate and stimulate Aβ significantly faster than membranes containing only non-oxidized or saturated phospholipids. When characterized the conformation, orientation, and rate of accumulation of the protein on various lipid membrane models. However, in all LS treated groups, the dramatic increase in both $svCH_2$ area, HBW and the shift to the higher frequencies may be attributed to the increase in gauche rotomers content than trans rotomers. The increase in lipid polarity and the unexpectedly increase in membrane fluidity may be due to LS antioxidant action. These results provide an insight on LS membrane interaction and suggest that LS can induce membrane disordering. From a physiological aspect, this disorder may be a good advantageous of LS because the interaction of antioxidants with lipid radicals would be more efficient when membrane lipids are more disordered [36].

Lipid peroxidation observed in AD human, mice and rat brain tissues suggesting that antioxidant defenses are impaired in AD subjects [43].

The noticeable increase in the A(3012 cm^{-1})/A(2956 cm^{-1}) ratio for the AD group compared to the control may indicate of degradation of the fatty acids to shorter chain due to AD oxidative stress. However, opposite results were obtained by [6].

Treating AD rats with LS water extract further increase the olefinic sub-band area for both the curative and protective groups that may be due to the elevated degree of the phospholipids unsaturation due to the LS antioxidant effect. However, for LS healthy group this area increased indeed but not to that extent as the curative and protective groups. However, both curative and protective groups are already diseased tissues but receiving a high dose of LS water extract that contains high amount of antioxidants and free radical scavengers. Thus, ATR-IR detected mutually the unsaturated trans fatty acids due to accumulation of lipid peroxidation end products and gauche rotomers polyunsaturated fatty acids due of treatment with LS. This is evident by the moderate elevation of the olefinic band area for LS group only and the calculated A (3012 cm^{-1})/A (2952 cm^{-1}) ratio.

The noticed increase in the membrane polarity, fluidity and the acyl chain packing in the curative group compared to the $AlCl_3$ are due to the hydrophobic part of LS. This part could be mainly due to the aromatic ring in the phenolic compounds, enter the non-polar part of the membrane and hence increasing the membrane disorder and fluidity by increasing of methylene gauche conformers [36]. Thus, these results strongly suggest that membrane phospholipids of rat hippocampus tissue undergo free radical attacks caused by oxidative stress mediated by $AlCl_3$. $AlCl_3$ primary affects the polyunsaturated fatty acids rendering them to transform rather than gauche rotomers with degradation of hydrocarbon chain to shorter chain length. The increased in membrane fluidity and membrane disorder is now due to the presence of Aβ proteins that disrupted the membrane structure. Meanwhile, the study proved in addition a promising therapeutic effect of LS on AD rat model that reduces the signs of oxidative stress on both membrane lipid peroxidation and the changes in protein conformation (will be discussed in full details in the extended version of this paper). These findings are greatly supported by the results obtained from the light microscope that will be explained at the end of this discussion.

ATR-IR is a sensitive technique, which can detect the alteration in the protein secondary structure and protein aggregation *in vivo* and *in vitro*. By using the second derivative and curve fitting analysis protein secondary structure could be studied qualitatively and quantitatively. It was believed that the misfolding and aggregation of naturally occurring proteins in the body lead to many diseased including AD, Parkinson's disease, and Diabetes type II. The protein misfolding is without doubt associated with a change in the protein secondary structure. Kawahara and Kato-Negishi [7] explained in an extensive review article that Al when bind to proteins can cause proteins oligomerization and induces a conformational changes that in turn can inhibit protein degradation by proteases. These aggregations may disrupt the cellular membrane and cell function leading to cell death [44].

In this study, the marked increase in the β-sheet parallel and antiparallel protein sub-bands around 1672 cm^{-1}, 1695 cm^{-1} respectively together with the observed band shifts in the $AlCl_3$ group compared to the control may be due to the oxidation of proteins and the formation of the characteristic

Aβ structure of AD. Treating AD rats with LS water extract reduces this protein values to a great extent to approach the control values (data not shown).

Aβ would appear to increase the membrane rigidity but in fact, it has been reported that it increases the membrane disorder and/or the membrane fluidity [45], [46].

Aβ can disrupt the membrane fluidity, which can contribute to the disruption in different cell functions such as calcium signaling, and lipid transport [38]-[40].

Müller et al. [47] reported that the peptide fragment Aβ 25-35 reduced fluidity and increased anisotropy of mouse and rat brain membranes. Consequently, the membrane polarity would increase too.

There are no agreement on effects of Aβ proteins on the membrane fluidity which may be due to tissue source and preparation, and if Aβ is soluble or insoluble.

Many studies reported that in AD the hippocampal and cortical pyramidal neurons showed reduced dendritic branching and length in patients [47], [48], and in animal models as well [47]-[50]. This reduction in dendritic branching and length would render neurons more compact [51]. In these compact neurons, the synaptic currents may transferred into the postsynaptic more efficiently and increasing the axosomatic depolarization as well. Thus, in turn is increased the action potential output [52]. Consequently, hyper excitability and abnormal circuit synchronization take place which are greatly contributing to cognitive dysfunction in patients and animal models of AD [53]-[56]. The relation between structural degradation of dendritic region and the neuronal hyper excitability was studied by [51] in a transgenic mouse model. They found that the average action potential frequency during spontaneous firing was increased by 62%. Many studies attributed the increase in network excitability in AD animals to the Aβ toxicity that disturb membrane lipid and membrane potential [54]. Ca^{++} in both hippocampus and cortex plays a significant role in AD mouse hyper excitability evident by an increase rate of Ca^{++} transients that was prevented by treating animals with γ-secretase inhibitor [54], [57]. These findings were consistent with the results obtained from this study, by observation of $AlCl_3$ AD group, rat were extremely aggressive than the other tested group and by light microscope micrographs. Al markedly degenerate the hippocampal neurons in $AlCl_3$ group as most cells appeared small, shrieked, and deformed. While, the number of degenerated cells upon Al intoxication decrease significantly in all LS treated groups and appeared with less intensity when stained with congo red. For curative and protective groups, the hippocampal neurons appeared nearly like the control.

V. Conclusion

To conclude, ATR-IR spectroscopy succeeded in determination the lipid peroxidation and protein oxidation due to oxidative damage induced by $AlCl_3$ in AD hippocampus rat brain. The lipid membrane polarity, ordering, the hydrocarbon chain length, the degree of saturation/ unsaturation, the total lipid to protein ratio and the alteration in the conformational protein structure all these parameters gave a deep insight into the role of Al in AD pathogenesis. In addition, it was powerful technique for the assessment of the curative and protective effect of LS water extract, as anti-AD aspect, which could give excellent anticipation in future in treating AD. Taking into consideration the close relationship between structural changes and disturbance of single neuron excitability and network malfunction, keeping neural structure integrities unchanged is an important target in designing preventive and/or therapeutic strategies [51]. Thus, LS water extract showed beneficial effects in treating AD.

The exact role of LS in treating AD and its major active ingredient will be discussed in our next work. However, further investigation should be carried to complete this study and to assess this new safely therapeutic drug for humans.

Acknowledgment

This research work was supported by King Abdulaziz City for Science and Technology; grant number: AT-145-34.

References

[1] N. A. Yassin, S. M. El-Shenawy, K. A. Mahdy, N. A. Gouda, A. E. Marrie, A. R. Farrag, and B. M. Ibrahim, "Effect of Boswellia serrata on Alzheimer's disease induced in rats," *J Arab Soc Med Res,* vol. 8, pp. 1-11, March 2013.

[2] Alzheimer's-Association, "2014 Alzheimer's disease facts and figures," *Alzheimer's & Dementia,* vol. 10, no. 2, pp. e47-e92, March 2014.

[3] Alzheimer's Disease International. About Alzheimer's disease. (Accessed December 14, (2005) at http://www.alz.co.uk/ alzheimers/faq.html#howmany).

[4] N. Braidy, A. Poljak, C. Marjo, H. Rutlidge, A. Rich, T. Jayasena, N. C. Inestrosa, and P. Sachdev, "Metal and complementary molecular bioimaging in Alzheimer's disease," *Front Aging Neurosci.,* vol. 6, no. 138, pp. 1-14, July 2014.

[5] Bukowska, "Toxicity of 2, 4-dichlorophenoxyacetic acid – molecular mechanisms," *Polish J. of Environ. Stud.,* vol. 15, no. 3, pp. 365-374, 2006.

[6] G. Cakmak, F. Zorlu, M. Severcan, and F. Severcan, "Screening of protective effect of amifostine on radiation-induced structural and functional variations in rat liver microsomal membranes by FT-IR spectroscopy," *Analytical chemistry,* vol. 83, no. 7, pp. 2438-2444, 2011.

[7] M. Kawahara and M. Kato-Negishi, "Link between aluminum and the pathogenesis of Alzheimer's disease: the integration of the aluminum and amyloid cascade hypotheses," *International Journal of Alzheimer's Disease,* vol. 2011, pp. 1-17, January 2011.

[8] A. Shati, F. G. Elsaid, and E. E. Hafez, "Biochemical and molecular aspects of aluminium chloride-induced neurotoxicity in mice and the protective role of Crocus sativus L. extraction and honey syrup," *Neuroscience,* vol. 175, no. null, pp. 66-74, 2011.

[9] P. Sethi, A. Jyoti, R. Singh, E. Hussain, and D. Sharma, "Aluminium-induced electrophysiological, biochemical and cognitive modifications in the hippocampus of aging rats," *NeuroToxicology,* vol. 29, no. 6, pp. 1069–1079, November 2008.

[10] P. Y. Niu, Q. Niu, Q. L. Zhang, L. P. Wang, S. E. He, T. C. Wu, P. Conti, M. Di-Gioacchino, and P. Boscolo, "uminum impairs rat neural cell mitochondria in vitro," *Int. J. Immunopathol. Pharmacol,* vol. 18, pp. 683–689, October 2005.

[11] Kumar, A. Bal, and K. D. Gill, "Impairment of mitochondrial energy metabolism in different regions of rat brain following chronic exposure to aluminium," *Brain Res.,* vol. 1232, no., pp. 94–103, September 2008.

[12] V. Kumar, A. Bal, and K. D. Gill, "Susceptibility of mitochondrial superoxide dismutase to aluminium induced oxidative damage," *Toxicology,* vol. 255, no. 3, pp. 117–123, January 2009.

[13] V. Kumar, A. Bal, and K. D. Gill, "Aluminium-induced oxidative DNA damage recognition and cell-cycle disruption in different regions of rat brain," *Toxicology,* vol. 264, no. 3, pp. 137–144, October 2009.

[14] J. L. Esparza, M. Gómez, M. Rosa Nogues, J. L. Paternain, J. Mallol, and J. L. Domingo, "Melatonin reduces oxidative stress and increases gene expression in the cerebral cortex and cerebellum of aluminum-

exposed rats," *Journal of pineal research,* vol. 39, no. 2, pp. 129-136, September 2005.

[15] H. C. Lee and Y. H. Wei, "Oxidative stress, mitochondrial DNA mutation, and apoptosis in aging," *Experimental biology and medicine,* vol. 232, no. 5, pp. 592-606, May 2007.

[16] A. Moshtaghie, "Aluminium administration on acetylcholinesterase activity of different regions of rat brain," *Med J Islamic Acad Sci,* vol. 12, pp. 105–108, 1999.

[17] Szutowiicz, H. Bielarcczyk, Y. Kisielevski, A. Jankowska, B. Madziar, and M. Tomaszewicz, "Effects of aluminium and calcium on acetyl-CoA metabolism in rat brain mitochondria," *J Neurochem,* vol. 71, no. 6, pp. 2447–2453, December 1998.

[18] R. Pan, S. Qiu, D. X. Lu, and J. Dong, "Curcumin improves learning and memory ability and its neuroprotective mechanism in mice," *Chinese Medical Journal (English Edition),* vol. 121, no. 9, pp. 832-839, 2008.

[19] L. A. Daiello, E. K. Festam, B. R. Ott, and W. C. Heindel, "Cholinesterase inhibitors improve visual attention in drivers with Alzheimer's disease," *Alzheimers Dement,* vol. 4, no. 4, pp. T498, 2008.

[20] F. Conforti, S. Sosa, M. Marrelli, F. Menichini, G. A. Statti, D. Uzunov, A. Tubaro, and F. Menichini, "The protective ability of mediterranean dietary plants against the oxidative damage: The role of radical oxygen species in inflammation and the polyphenol, flavonoid and sterol contents," *Food Chemistry,* vol. 112, no. 3, pp. 587-594, February 2009.

[21] S. R. Mentreddy, "Medicinal plant species with potential antidiabetic properties. Journal of the Science of Food and Agriculture," *Journal of the Science of Food and Agriculture,* vol. 87, no. 5, pp. 743-750, April 2007.

[22] R. Drury and E. Wallington, *Carleton's histological technique*, 5th ed. Oxford: Oxford University Press, 1980, pp. 188–291.

[23] J. D. Banchroft, A. Stevens, and D. R. Turner, *Theory and Practice of Histological Techniques*, 4th ed. New York: Churchill Livingstone, 1996.

[24] V. Kumar and K. D. Gill, "Oxidative stress and mitochondrial dysfunction in aluminium neurotoxicity and its amelioration: a review," *NeuroToxicology,* vol. 41, pp. 154-166, March 2014.

[25] H. L. Casal and H. H. Mantsch, "Polymorphic phase behaviour of phospholipid membranes studied by infrared spectroscopy," Biochim Biophys Acta, vol. 779, no. 4, pp. 381-401, December 1984.

[26] P. Axelsen, H. Komatsu, and I. Murray, "oxidative stress and cell membranes in the pathogenesis of Alzheimer's disease," *Physiology,* vol. 26, no. 1, pp. 54-69, February 2011.

[27] Gella and I. Bolea, "Oxidative stress in Alzheimer's disease: pathogenesis, biomarkers and therapy," in *Alzheimer's disease pathogenesis-core concepts, shifting paradigms and therapeutic targets*, Rijeka, Croatia: InTech, 2011, pp. 319-344.

[28] N. S. Selim, O. S. Desouky, N. M. smail, and A. Z. Dakrory, "Spectroscopic analysis of irradiated erythrocytes," *Radiation Physics and Chemistry,* vol. 80, no. 12, pp. 1337-1342, December 2011.

[29] G. Cakmak, L. M. Miller, F. Zorlu, and F. Severcan, "Amifostine, a radioprotectant agent, protects rat brain tissue lipids against ionizing radiation induced damage: an FTIR microspectroscopic imaging study," *Archives of biochemistry and biophysics,* vol. 520, no. 2, pp. 67-73, April 2012.

[30] S. Khouw, S. Parthasarathy, and J. L. Witztum, "Radioiodination of low density lipoprotein initiates lipid peroxidation: protection by use of antioxidants," *Journal of lipid research,* vol. 34, no. 9, pp. 1483-1496, September 1993.

[31] L. L. de Zwart, J. H. Meerman, J. N. Commandeur, and N. P. Vermeulen, "Biomarkers of free radical damage: applications in experimental animals and in humans," *Free Radical Biology and Medicine,* vol. 26, no. 1-2, pp. 202-226, January 1999.

[32] K. Z. Liu, R. Bose, and H. H. Mantsch, "Infrared spectroscopic study of diabetic platelets," *Vibrational spectroscopy,* vol. 28, no. 1, pp. 131-136, February 2002.

[33] H. Yin, L. Xu, and N. A. Porter, "Free radical lipid peroxidation: mechanisms and analysis," *Chemical reviews,* vol. 111, no. 10, pp. 5944-5972, August 2011.

[34] O. P. Lamba, M. C. Y. Sundeep Lal, M. F. Lou, and D. Borchman., "Spectroscopic detection of lipid peroxidation products and structural changes in a sphingomyelin model system," *Biochimica et Biophysica Acta,* vol. 1081, no. 2, pp. 181-187, January 1991.

[35] M. V. Fraile, B. Patrón-Gallardo, G. López-Rodríguez, and P. Carmonab, "FT-IR study of multilamellar lipid dispersions containing cholesteryl linoleate and dipalmitoylphosphatidylcholine," *Chemistry and Physics of Lipids,* vol. 97, no. 2, pp. 119-128, February 1999.

[36] Borchman, F. Giblin, V. Leverenz, V. Reddy, L. Li-Ren, M. Yappert, D. Tang, and L. Li, "Impact of aging and hyperbaric oxygen in vivo on guinea pig lens lipids and nuclear light scatter," *Invest Ophthalmol Vis Sci.,* vol. 41, no. 10, pp. 3061–3073, September 2000.

[37] Borchman, G. N. Foulks, M. C. Yappert, J. Bell, E. Wells, S. Neravetla, and V. Greenstone, "Human meibum lipid conformation and thermodynamic changes with meibomian-gland dysfunction," *Investigative ophthalmology & visual science,* vol. 52, no. 6, pp. 3805–3817, May 2011.

[38] N. Arispe, E. Rojas, and H. B. Pollard, "Alzheimer disease amyloid beta protein forms calcium channels in bilayer membranes: blockade by tromethamine and aluminum," *Proceedings of the National Academy of Sciences,* vol. 90, no. 2, pp. 567–571, January 1993

[39] J. McLaurin and A. Chakrabartty, "Membrane disruption by alzheimer β-amyloid peptides mediated through specific binding to either phospholipids or gangliosides implications for neurotoxicity," *Journal of Biological Chemistry,* vol. 271, pp. 26482-26489, October 1996

[40] H. Hartmann, A. Eckert, and W. E. Muller, "Apolipoprotein E and cholesterol affect neuronal calcium signaling: the possible relationship to β-amyloid neurotoxicity," *Biochemical and biophysical research communications,* vol. 200, no. 3, pp. 1185-1192, May 1994.

[41] L. M. Miller, M. W. Bourassa, and R. J. Smith, "FTIR spectroscopic imaging of protein aggregation in living cells," *Biochimica et Biophysica Acta (BBA) - Biomembranes,* vol. 1828, no. 10, pp. 2339-2346, October 2013.

[42] V. Koppaka and P. H. Axelsen, "Accelerated accumulation of amyloid β proteins on oxidatively damaged lipid membranes," *Biochemistry,* vol. 39, no. 32, pp. 10011-10016, August 2000.

[43] M. A. Lovell, W. D. Ehmann, S. M. Butler, and W. R. Markesbery, "Elevated thiobarbituric acid-reactive substances and antioxidant enzyme activity in the brain in Alzheimer's disease," *Neurology,* vol. 45, no. 8, pp. 1594-1601, August 1995.

[44] M. Ramirez-Alvarado, J. W. Kelly, and C. M. Dobson, *Protein misfolding diseases: Current and emerging principles and therapies* vol. 14. New York: John Wiley & Sons, 2010.

[45] N. A. Avdulov, S. V. Chochina, U. Igbavboa, E. O. O'Hare, F. Schroeder, J. P. Cleary, and W. G. Wood, "Amyloid β-Peptides Increase Annular and Bulk Fluidity and Induce Lipid Peroxidation in Brain Synaptic Plasma Membranes," *Journal of neurochemistry,* vol. 68, no. 5, pp. 2086-2091, May 1997.

[46] S. V. Chochina, N. A. Avdulov, U. Igbavboa, J. P. Cleary, E. O. O'Hare, and W. G. Wood, "Amyloid β-peptide1-40 increases neuronal membrane fluidity: role of cholesterol and brain region," *Journal of lipid Research,* vol. 42, no. 8, pp. 1292-1297, August 2001.

[47] T. L. Spires and B. T. Hyman, "Neuronal structure is altered by amyloid plaques," *Rev. Neurosci,* vol. 15, no. 4, pp. 267–278, August 2004.

[48] J. Grutzendler, K. Helmin, J. Tsai, and W. B. Gan, "Various dendritic abnormalities are associated with fibrillar amyloid deposits in Alzheimer's disease," *Ann. N Y Acad. Sci.,* vol. 1097, pp. 30–39, February 2007.

[49] D. L. Moolman, O. V. Vitolo, J. P. Vonsattel, and M. L. Shelanski, "Dendrite and dendritic spine alterations in Alzheimer models," *J. Neurocytol,* vol. 33, no. 3, pp. 377–387, May 2004.

[50] J. Tsai, J. Grutzendler, K. Duff, and W. B. Gan, "Fibrillar amyloid deposition leads to local synaptic abnormalities and breakage of neuronal branches," *Nat. Neurosci,* vol. 7, pp. 1181–1183, October 2004.

[51] Z. Šišková, D. Justus, H. Kaneko, D. Friedrichs, N. Henneberg, T. Beutel, J. Pitsch, S. Schoch, A. Becker, H. v. d. Kammer, and S. RemyRemy, "Dendritic structural degeneration is functionally linked to cellular hyperexcitability in a mouse model of Alzheimer's disease," *Neuron,* vol. 84, no. 5, pp. 1023-1033, December 2014.

[52] D. Johnston, J. C. Magee, C. M. Colbert, and B. R. Cristie, "Activeproperties of neuronal dendrites," *Annu. Rev. Neurosci,* vol. 19, no., pp. 165–186, 1996.

[53] J. J. Palop, J. Chin, E. D. Roberson, J. Wang, M. T. Thwin, N. Bien-Ly, J. Yoo, K. O. Ho, G. Q. Yu, A. Kreitzer, S. Finkbeiner, J. L. Noebels, and L. Mucke, "Aberrant excitatory neuronal activity and compensatory remodeling of inhibitory hippocampal circuits in mouse models of Alzheimer's disease," *Neuron,* vol. 55, no. 5, pp. 697–711, September 2007.

[54] M. A. Busche, G. Eichhoff, H. Adelsberger, D. Abramowski, K. H. Wiederhold, C. Haass, M. Staufenbiel, A. Konnerth, and O. Garaschuk, "Clusters of hyperactive neurons near amyloid plaques in a mouse model

of Alzheimer's disease," *Science,* vol. 321, no. 5896, pp. 1686–1689, September 2008.

[55] P. E. Sanchez, L. Zhu, L. Verret, K. A. Vossel, A. G. Orr, J. R. Cirrito, N. Devidze, K. Ho, G. Q. Yu, J. J. Palop, and L. Mucke, "Levetiracetam suppresses neuronal network dysfunction and reverses synaptic and cognitive deficits in an Alzheimer's disease model," *Proc. Natl. Acad. Sci. USA* vol. 109, no. 42, pp. E2895–E2903, October 2012

[56] K. A. Vossel, A. J. Beagle, G. D. Rabinovici, H. Shu, S. E. Lee, G. Naasan, M. Hegde, S. B. Cornes, M. L. Henry, A. B. Nelson, W. W. Seeley, M. D. Geschwind, M. L. Gorno-Tempini, T. Shih, H. E. Kirsch, P. A. Garcia, B. L. Miller, and L. Mucke, "Seizures and epileptiform activity in the early stages of Alzheimer disease," *J. Am. Med. Assoc. neurology,* vol. 70, no. 9, pp. 1158–1166, September 2013.

[57] M. A. Busche, X. Chen, H. A. Henning, J. Reichwald, M. Staufenbiel, B. Sakmann, and A. Konnerth, "Critical role of soluble amyloid-b for early hippocampal hyperactivity in a mouse model of Alzheimer's disease," *Proc. Natl. Acad. Sci. USA,* vol. 109, no. 22, pp. 8740–8745, May 2012.